EFDA–JET–CP(14)06/25

E. de la Luna, P. Lomas, S. Saarelma, I. Nunes, L. Frassinetti, S. Bresinzek, S. Weisen, M. Beurskens, J. Flanagan, M. Groth, A. Loarte, F. Nave, V. Parail, F. Rimini, G. Saibene, R. Sartori, G. Sips, M. Stamp, E.R. Solano, H. Urano and JET EFDA contributors

Comparative Study of High Triangularity H-mode Plasma Performance in JET with Be/W Wall and CFC Wall

Comparative Study of High Triangularity H-mode Plasma Performance in JET with Be/W Wall and CFC Wall

E. de la Luna[1], P. Lomas[2], S. Saarelma[2], I. Nunes[3], L. Frassinetti[4], S. Bresinzek[5], S. Weisen[5], M. Beurskens[2], J. Flanagan[2], M. Groth[6], A. Loarte[7], F. Nave[3], V. Parail[2], F. Rimini[2], G. Saibene[8], R. Sartori[8], G. Sips[9], M. Stamp[2], E.R. Solano[1], H. Urano[10] and JET EFDA contributors*

JET-EFDA, Culham Science Centre, OX14 3DB, Abingdon, UK

[1]Laboratorio Nacional de Fusion, CIEMAT, 28040, Madrid, Spain
[2]CCFE Fusion Association, Culham Science Centre, OX14 3DB, Abingdon, OXON, UK
[3]IST, Instituto de Plasmas e Fusão Nuclear, Av Rovisco Pais, 1049-001, Lisbon, Portugal
[4]Division of Fusion Plasma Physics, AKTH, SE-10044 Stockholm, Sweden
[5]Institut fur Energie- und Klimaforschung - Plasmaphysik, Forschungszentrum Julich, Germany
[6]AaltoUniversity, Association EURATOM-Tekes, Espoo, Finland
[7]ITER Organization, Route de Vinon sur Verdon, 13115 St. Paul Lez Durance, France
[8]Fusion for Energy, Joint Undertaking, 08019 Barcelona, Spain
[9]European Commission, B-1049 Brussels, Belgium
[10]Japan Atomic Energy Agency, Naka Fusion Institute, Ibaraki, 311-0193, Japan
** See annex of F. Romanelli et al, "Overview of JET Results", (25th IAEA Fusion Energy Conference, St Petersburg, Russia (2014)).*

Preprint of Paper to be submitted for publication in Proceedings of the
25th IAEA Fusion Energy Conference, St Petersburg, Russia
13th October 2014 - 18th October 2014

ABSTRACT

A series of experiments has been conducted in JET-ILW to investigate the low performance (with $H_{98} < 0.8$) of the H-modes plasmas at high triangularity, mainly due to increased pedestal degradation at high density. The study includes variations of the core shape and the divertor geometry to explore the impact of recycling and divertor pumping on pedestal parameters and ELM characteristics. Unlike in JET-C, high density H-mode plasmas in JET-ILW, independently of their triangularity, show signs of a very cold and dense neutral cloud in the inner divertor, with the appearance of 'inverted' ELMs typically associated to inter ELM partial detachment. This reflects the different divertor recycling patterns associated with the change in wall materials.

1. INTRODUCTION

One of the key challenges for the existing ITER Q = 10 ITER baseline scenario is the requirement to achieve good confinement (with $H_{98} \sim 1$, defined by the IPB98(y,2) scaling) at sufficiently high density ($n_e \geq 0.85 \times n_{GW}$, where n_{GW} is the Greenwald density). In JET-C (with CFC plasma facing components), the best performance in terms of H_{98} was obtained in unfuelled type I ELMy H-modes and the confinement was generally degraded at increasing D fuelling levels[1]. Raising the plasma triangularity was the only effective way found to increase the plasma density without reducing the confinement and similar results were obtained in other tokamaks (e.g. AUG[2], DIII-D[3]). Indeed, near-stationary H-mode plasmas with good confinement ($H_{98} > 0.9$) at $n_e \sim n_{GW}$ were reproducibly obtained in JET-C in high triangularity (high-δ) configurations ($\delta > 0.4$)[1,4]. The situation is somewhat different in JET with the new ITER-like wall (ILW). The use of a moderately large gas puffing ($> 10^{22}$ D/s) to keep the core radiation within acceptable limits has become a necessity in ILW operation and typically $H_{98} < 0.9$[5]. The first experimental campaign in JET-ILW showed that whilst the degradation of confinement with gas fuelling at low triangularity appeared to be compatible with that measured in JET-C, the positive influence of triangularity on confinement was not recovered in the baseline ELMy H-mode plasmas due to increased pedestal degradation at high density [4,5]. Confinement in high-δ plasmas could be partially recovered by N_2 seeding[4]. The investigation of the baseline scenario in JET-ILW has continued in 2013 and 2014. Recent experiments have shown the beneficial effects of increased divertor pumping in achieving good confinement in JET-ILW[6,7,8]. A more efficient pumping can be achieved by locating both strike points in the divertor corners, enabling the production of steady-state ELMy H-mode plasmas at 2–2.5MA with good energy confinement ($H_{98} \sim 1$ and $\beta_N \sim 1.8$–2), which represents a significant improvement with respect to the best steady state performance reported in the last IAEA conference. So far, the positive impact of pumping on confinement has been only demonstrated at low-δ.

This paper reports on the status of an ongoing investigation to understand the mechanism responsible for the lower confinement obtained in high-δ ELMy H-mode plasmas compared to JET-C experiments. To this purpose, dedicated experiments, with variations of the core shape and the divertor geometry, were performed to explore the impact of recycling and divertor pumping

on ELMs and pedestal parameters in high-δ JET-ILW H-mode plasmas. In addition, systematic comparisons of an extended database of JET-C and JET-ILW discharges are carried out to study the specific properties of the high δ H-mode plasmas and identify the key differences between the two datasets. We will also briefly address the peeling-ballooning mode stability analysis for high-δ plasmas in the context of the results presented here.

2. EFFECT OF MAGNETIC TOPOLOGY (CORE & DIVERTOR) ON CONFINEMENT IN JET-ILW

Following the encouraging results obtained with improved divertor pumping at low-δ ($\delta_{av} = 0.2$) [6,7], experiments were carried out using a high triangularity ($\delta_{av} = 0.38$) configuration with the outer strike point located close to the pump duct entrance. The different divertor geometries used in the experiments reported here are shown in Figure 1 together with the configuration naming convention adopted in this paper. In the earlier JETILW campaigns, the outer strike point was on the horizontal target in the majority of the high-δ discharges.

The results of this experiment, summarized in Figure 2, are compared to the results reported in the last IAEA [5] (including JET-C discharges and JET-ILW discharges from 2011–2012 experiments). The low-δ discharges used here represent a subset of a larger database reported in [8], at constant plasma current ($I_p = 2.5$MA) and various toroidal fields (2.5–2.7T), heated with 14–20MW of NBI power (2–3MW of ICRH). The data shown are obtained from the steady ELMy phase of each discharge, averaged over at least 1 sec ($\sim 3\tau_E$). D_2 gas puffing is used for W accumulation control in all the JET-ILW discharges, while the low-δ JET-C data shown in Figure 2 are unfuelled. As seen in Figure 2(a), the H_{98} factor is on average ~ 0.9-1 for the low-δ configuration with both strikes points on the divertor corners (CC/LT) and ~ 0.75 for the rest of the divertor geometries, independently of triangularity. Figure 2(b) shows how the more efficient pumping of the divertor corner configuration has significantly widened the operational space of the ELMy H-mode plasmas in JET-ILW towards lower $n_{e,ped}$ and higher $T_{e,ped}$, with $T_{e,ped}$ 1–1.2keV and $n_{e,ped}/n_{GDL} = 0.4$-0.5, as compared to the initial JETILW operation [5], with $T_{e,ped} < 0.8$keV and $n_{e,ped}/n_{GDL} = 0.6$-0.8. This has allowed to extend down the range of achievable edge collisionalities, from $\nu_e^* \sim 0.5$–1 to ~ 0.2. The increase in $T_{e,ped}$ seen in the CC/LT configuration is accompanied by an increase in the core temperatures (both T_e and T_i), as expected for stiff temperature profiles, resulting in higher stored energy for similar input power and therefore higher confinement. With increasing density, obtained by gas injection and/or reduced pumping, a marked reduction in performance (stored energy, H_{98} and β_N) is clearly seen, for both high and low triangularity. A more detailed analysis of the impact of divertor geometry on global confinement using a different dataset is given in a companion paper[6]. At the lowest fuelling rates (low plasma density) the energy confinement time of the CC/LT discharges (with $H_{98} = 0.9$–1.1 and $\beta_N = 1.8$–2) is similar to that obtained in unfuelled low-δ H-mode plasmas in JET-C. In contrast, there is little difference, in either the confinement or the attainable density, in high-δ discharges when the outer strike point was moved closer to the pumping duct (VH/HT→VC/HT)

for a wide range of operating conditions ($\Gamma_D \sim 2–5 \times 10^{22}$ e/s, $P_{NBI} = 15–20$MW). As reported earlier [4,5], the pedestal density values of the high-δ plasma in JET-ILW are similar to those obtained in JET-C but $T_{e,ped}$ is substantially lower, as a consequence the confinement ($H_{98} \leq 0.8$, $\beta_N \leq 1.5$) is strongly reduced to values close to those measured in the type III ELM regime in JET-C.

3. INFLUENCE OF PUMPING ON H-MODE CONFINEMENT AT HIGH δ IN JET-C

Given that the majority of the divertor pumping in JET is carried out by the outer section of the divertor (closer to the cryopump), it was somewhat surprising the lack of pedestal density variation obtained in high-δ JET-ILW plasmas when the outer strike point was moved close to the pumping duct. It is thus of interest to compare the plasma response to changes in pumping in high-δ discharges in JET-C. In order to do that, we concentrate on a set of dedicated gas scans ($\Gamma_D = 0.2\text{-}9 \times 10^{22}$e/s) performed in 2008 designed to compare the behaviour of the high δ ELMy H-mode plasmas (2.5MA, $q_{95} = 3.4$, $P_{NBI} \approx 15–18$MW) in three configurations with similar core shape ($\delta_{av} \approx 0.4$) but different divertor geometry, in which the outer strike point was located at increasing distances from the pump duct entrance to decrease pumping and expose its influence on plasma performance. The results of this experiment are summarized in Figure 3. Divertor fuelling was used in all the discharges. Different symbols denote different divertor geometries (see Figure 1). A similar gas scan carried out in 2003 [9] is also shown to illustrate the reproducibility of this type of experiments in JET-C. The difference in stored energy in the 2003 and 2008 scan is mostly due to the different input power used.

Similar behaviour was seen for the three divertor geometries. The plasma density increased at first as the gas fuelling was raised but eventually a maximum density was reached beyond which a strong deterioration of energy and particle confinement was found. Any further attempt to increase the density came at a price of a loss in confinement, the edge cooled down, density decreased and the ELMs became more compound until stationary Type III ELMy phases were obtained (with $H_{98} < 0.8$). As discussed in detail in previous publications [1,4], at $n_e \sim n_{GW}$ a reduction in the ELM frequency was observed (from 20 to 10Hz), which is typically associated to a transition to the mixed TypeI/II ELM regime. As can be seen in Figure 4, additional pumping has no effect on the achieved confinement at high density ($H_{98} \geq 0.9$ at $n_e \sim n_{GW}$ in all cases) other than by changing the edge density for a given neutral flux. As a consequence, the gas injection rates required for reaching the Greenwald density were a factor of 5 higher in the configuration with better pumping. However, a clear difference was found for the configuration with the lowest pumping (VH+/HT, with the largest distance between the outer strike point and the pump duct entrance), and hence lower Te,ped and higher ne,ped at low fuelling, where the achievement of good confinement was restricted to a very narrow gas rate range ($\Gamma_D < 0.7 \times 10^{22}$e/s). In this configuration (VH+/HT), Te,ped (not shown) decreases rapidly with increasing gas fuelling, and, as a consequence, smaller stored energy (up to 20%) is achieved for similar gas injection rates and input power. In contrast, with sufficient pumping, Te,ped can be maintained sufficiently high ($T_{e,ped} \geq 0.8$keV in this dataset) during the gas scan, shifting the confinement degradation observed close to the transition to type III

ELMs[1] to higher densities. The pedestal parameters of the divertor configuration with the lowest pumping efficiency resemble closely those observed in JET-ILW discharges. There is, however, a notable difference in the ELM behaviour seen in the JET-C and JET-ILW dataset. In JET-C the degradation in confinement was always associated to a transition to compound ELMs, with large ELMs followed by trains of faster and smaller ELMs, and to type III ELMs (with $f_{ELM} > 100$Hz) at the highest gas injection rate. However, in the case of the JET-ILW, $H_{98} < 0.8$ values are obtained for similar pedestal parameters but at rather low ELM frequencies ($f_{ELM} = 15–30$Hz) [10]. The ELM behaviour in JET-ILW will be discussed in the next section.

4. IMPACT OF RECYCLING ON ELMS AND CONFINEMENT IN JET-ILW

In JET/ILW gas puffing is used to increase the ELM frequency (f_{ELM}) to frequencies above 20–30Hz (depending on the input power and plasma conditions) and prevent the increase of W concentration in the core region[11], which otherwise may lead to a central radiative collapse. Gas puffing also contributes to reduce the W sputtering by reducing the temperature in the divertor target[12]. The use of gas fuelling has therefore become an essential operational tool in JET-ILW to access stable conditions, but it also reduces the energy confinement. Within the usual type I ELM phenomenology, the cooling down of the pedestal obtained by adding gas puffing is typically linked to smaller and faster ELMs (except for the mixed TypeI/II ELMs mentioned in the previous section). Surprisingly, the situation is somewhat different in JET-ILW.

This is illustrated in Figure 4 where the ELM frequency (f_{ELM}) is plotted against the gas injection rate (only discharges with divertor fuelling are shown here). We see the usual tendency of the f_{ELM} to increase with increasing gas puffing rates in the more recent low-δ plasmas at lower ne,ped (with $T_{e,ped} > 1$ keV). In contrast, for the high-δ discharges, and in general for high density discharges and lower $T_{e,ped}$ ($n_{e,ped} > 5\times10^{19}$m^{-3} and $T_{e,ped} < 0.8$keV in this dataset), f_{ELM} remains relatively low (15–30Hz) and very little variation is found in f_{ELM} with gas injection rate or input power [10]. Higher f_{ELM} were only observed at very high gas puffing rates. For comparison, data for a gas scan at high-δ in JETC is also displayed, showing the decrease in f_{ELM} characteristic of the access to type I/II ELMs and the subsequent transition to type III ELMs at higher gas puffing rates.

An example of the lack of increase of f_{ELM} with gas fuelling in JET-ILW is shown in figure 5, where a pair of matched discharges (2MA, 2.1T, low-δ with the strike points in the divertor corners, $P_{NBI} = 14$MW) with different gas injection level is displayed. The changes in confinement are similar to those described in Section 1. We find that the 30% increase in density causes a 15% reduction in the stored energy. In this case, the f_{ELM} is slightly higher in the discharge at lower gas level (34Hz in Pulse No: 85191 and 25Hz in Pulse No: 85192) for similar radiated power fraction ($P_{RAD}/P_{IN} \sim$ 30%). The plasma at the higher gas fuelling (Pulse No: 85191) and lower f_{ELM} remains stable for 2 sec, but the continued increase in radiation leads ultimately to a radiative collapse. However, the major difference between these two discharges is found in the ELM behavior as seen in the Dα emission from the inner divertor, which evolve into `inverted' ELMs [7,10] in the discharge with a

colder pedestal (Pulse No: 85191) and this is accompanied by a large increase in the Dα emission level. 'Inverted' ELMs typically refer to negative spikes at the ELM crash that are produced when a dense and cold ($T_e < 1–3eV$) plasma is viewed by the visible spectrometer, since then Dα is dominated by recombination. The burst of heat during the ELMs is of sufficient amplitude to burn through the cloud of neutrals, the Te close to the divertor target plate increases and the recombination rate drops, leading to a reduced Dα during the ELM crash [13].

The change in the ELM character seen in the high density JET-ILW plasmas (with $T_{e,ped} < 0.8$) is also observed in the time-scale of the pedestal collapse caused by the ELM, which can be significantly longer than in JET-C [5,14]. The different ELM behavior for plasmas at different $T_{e,ped}$ is illustrated in Figure 6 where measurements of the divertor Dα photon fluxes integrated across the inner and outer strike zone are shown for pulses with increasing ne,ped. The different ne,ped are obtained by reducing pumping through a change in the divertor configuration in a single discharge (Pulse No: 86533, CC/LT vsersus VH/LT) or increasing gas injection rate (Pulse No: 82540), in this case at high-δ (VH/HT). In addition the Te,ped and ne,ped evolution after the ELM crash are shown in the second column in Figure 6. The ECE channel closest to $\psi_{pol} \sim 0.95$ is used for T_e and the interferometer edge channel for n_e. The data are synchronized in order to have each ELM collapse at $t = 0$ and normalized to the pre-ELM value.

The time scale for the ELM collapse phase, characterized by the duration of the phase with strong broadband MHD activity, is in the region of 300–400μs for the JET-ILW ELMy discharges (not shown) and does not depend strongly on local pedestal conditions. Similar values were measured with the C-wall (200–300μs) [15]. However, while in JET-C the energy from the pedestal is lost within the first 300μs of the crash [15], in the case of JET-ILW plasmas the ELM duration (Δt_{ELM}) is on average longer, varying between 1 to 10ms [5,14] depending on pedestal parameters, being Δt_{ELM} the duration of the ELM crash as seen by the drop in the pedestal temperature. Similar results have been found in the analysis of the ELM induced transient heat load from fast infrared thermography[16].

As can be seen in the Figure 6, the rate of reduction in the temperature is initially fast in the three cases (with most of the $T_{e,ped}$ lost within < 2ms) but, for the discharge at higher $n_{e,ped}$, T_e and n_e can continue decreasing for up to 8ms. It is worth noting that ELMs with Δt_{ELM} of 2ms and 8ms can coexist in the same plasma for similar pedestal parameters [14], which clearly indicates that a physical mechanism unrelated to the MHD instability causing the ELM must be invoked to explain the slower time scale event seen after the ELM crash. The ELM energy losses for these slow events (with $\Delta t_{ELM} \geq 5$ ms) do not follow the inverse correlation of ELM size with pedestal collisionality typically seen for type I ELMs [15] and the relative ELM energy losses ($\Delta W_{ELM}/W_{ped}$, using kinetic profiles measurements) are a factor of 2 larger than in JET-C for similar edge ν_e^* [14]. The picture is very different at lower pedestal densities (higher Te,ped). In this case, the ELM behavior (ELM energy losses, width of the ELM affected volume and ELM crash duration) becomes again similar to that observed in JET-C. This can be seen in the low-δ pulses with improved pumping reported here

or in hybrid Hmode plasmas[17] (at $\beta_N > 2$), that typically operate at lower density (lower I_p) and lower gas injection rates. A more detailed description of the ELM losses for 'slow' and 'standard' type I ELMs can be found in [14]. The different ELM character in plasmas with different pedestal parameters is most clearly seen when looking at the response of the D_α signal to the heat flux arriving at the divertor after the ELM crash. The usual positive spikes associated to the ELMs typically found in JET-C plasmas can be seen in the inner and outer divertor D_α signals in the discharge at lower $n_{e,ped}$ and higher $T_{e,ped}$ (see Figure 6). In contrast, 'inverted' ELMs in the inner divertor are invariably seen in conditions of high neutral flux and low temperature in the divertor (plasmas with low $T_{e,ped}$). As shown in the Figure 6, the development of the slower transport events is only seen in the discharge with the highest pedestal density, typically associated to higher neutral fluxes. A novel hypothesis has been put forward recently [12] to explain the dynamics of the 'slow' ELMs based on a temporary change of the local recycling coefficient at the tungsten target plate directly after the heat pulse. The proposed physical explanation is that during the transient phase with $R < 1$ the W target plate behaves temporarily as a sink for the plasma, which would explain the strong reduction in D_α emission in the outer divertor at the time of the ELM crash as well as the second emission peak in D_α emission. More detailed analysis is planned to validate this hypothesis.

Unfortunately, the lack of diagnostic coverage in the case of the divertor corner configuration is a serious impediment for the detailed analysis of these discharges. The strike point location cannot be observed by the spectroscopic diagnostics and there are no Langmuir probes of infrared thermography data. Therefore, most of our information of the divertor characteristics is limited to the 'signature' of inter-ELM partial detachment, namely the enhanced baseline and the appearance of negative spikes in the inner divertor Dα signal, which are our best indicators of very cold, and dense divertor conditions. In addition, in the plasma conditions we have just described, the divertor radiation peak moves away from the divertor plate towards the inboard side of the X-point, which also a clear indication of low temperatures close to the divertor target. These observations clearly point to a much colder and denser divertor in the case of high-density H-mode plasmas with moderate to high gas fuelling (for both low and high triangularity) in JET-ILW than in comparable JET-C discharges.

5. PEELING-BALLOONING STABILITY ANALYSIS OF HIGH-Δ PLASMAS IN JET-ILW

Peeling-ballooning (P–B) stability analysis of the new dataset described in Section 1 confirm and extend earlier results from high density ELMy Hmodes plasmas in JET-ILW, where the pre-ELM pedestal in high-δ configurations at high gas fuelling, was seen to be stable to P–B modes [17]. Figure 7 compares the operating point within the stability diagram of one of the recent low ν_e^* discharges at low-δ (Pulse No: 85384, with $n_{e,ped} = 4.3 \times 10^{19} m^{-3}$, and $T_{e,ped} = 0.95$keV) and a high-δ discharge (Pulse No: 85385, with $n_{e,ped} = 6 \times 10^{19} m^{-3}$, and $T_{e,ped} = 0.75$keV) at the same I_p/B (2.5MA/2.7T), and similar heating power (20MW) and gas fuelling ($\Gamma_D \sim 3.5 \times 10^{22}$ e/s). While

the operating point just before an ELM occurs is above the stability boundary for P–B modes (for toroidal mode numbers in the range $3 < n < 70$) for the low-δ case, it resides in the stable regime of the P–B stability diagram for the high-δ case. The lower $T_{e,ped}$ measured in the high-δ discharge implies higher ν_e^* and smaller edge currents. As can be seen in Figure 7, these effects tend to shift the plasma edge toward the high-n ballooning branch, where the increased pedestal stability resulting from plasma shaping disappears[18].

The pedestal stability analysis of the JET-ILW hybrid plasmas support this idea, since in this scenario, which typically operate at lower ν_e^* and higher β_N, the beneficial effect of triangularity on confinement is recovered [17]. Additional effects may play a role in this case, because the improved stability for ballooning modes due to increased Shafranov-shift obtained at high β_N could also facilitate the access to the region of pedestal stability where the plasma shaping is the most effective at improving stability [19]. On the other hand, the basic picture proposed here is challenged by the ELM characteristics seen at high ν_e^* plasmas in JET-ILW. With reduced ∇Pe and low bootstrap current in the pedestal region, the main drivers for the triggering of the P–B modes, one would expect the appearance of small ELMs rather than the large ELMs seen at high ν_e^* plasmas in JET-ILW. Normally the P–B modes are considered to be an ideal MHD instability but resistivity may be involved in the case of the colder pedestal obtained in JET-ILW. An overview of the most recent edge stability studies performed in JET-ILW can be found in [20].

6. SUMMARY AND CONCLUSIONS

The best confinement results on JET-ILW have been obtained in low-δ H-mode plasmas with moderate gas fuelling and a divertor configuration optimal for pumping (with both strike points in the divertor corners) [6,7]. In those conditions, confinement as good as in unfuelled low-δ JET-C H-mode plasmas has been obtained. The impact of pumping on high triangularity plasma has also been examined in both JET-ILW and JET-C, but in this case only the outer divertor geometry was modified, while the inner strike point was kept in the divertor vertical plate. Whereas in JET-C access to lower ne,ped at a given gas injection rate was easily obtained by placing the outer strike point closer to the pumping duct, similar experiments carried out in JET-ILW did not show any significant impact in the confinement or the attainable density. Moreover, virtually all the JET-ILW discharges at high density ($n_{e,ped} > 5 \times 10^{19} m^{-3}$), obtained with gas puffing and/or reduced pumping, show signs of a very cold and dense neutral cloud in the inner divertor ('inverted' ELMs), independently of their triangularity. In those conditions, characterized by low $T_{e,ped}$ (< 0.8keV) and poor confinement ($H_{98} < 0.8$), longer ELM durations are found in JET-ILW (1–10ms) as compared to JET-C (< 0.5ms). The differences found between JET-C and JET-ILW H-mode plasmas suggests that the change in wall materials has strongly affected the divertor recycling patterns in gas fuelled JET-ILW H-mode plasmas, although the mechanisms responsible of these differences are still unknown. As discussed in [6], it was found experimentally that the energy confinement in JET-ILW depends on the divertor geometry and the resultant changes in the divertor plasma parameters but none of the possible

mechanisms investigated so far have been able to explain the strong degradation of confinement observed in JET-ILW with reduced pumping or increased gas injection and hence the question of why the pedestal in high density high-δ plasma is colder in JET-ILW than in JET-C remains open. Upcoming experiments are planned to continue investigating the confinement of high-δ plasmas in JET-ILW.

ACKNOWLEDGEMENTS

This work was supported by EURATOM and carried out within the framework of the European Fusion Development Agreement. The views and opinions expressed herein do not necessarily reflect those of the European Commission.

REFERENCES

[1]. G. Saibene et al (2002) Plasma Physics and Controlled Fusion **44** 1769
[2]. J. Stober et al (2000) Plasma Physics and Controlled Fusion **42** A211-215
[3]. T. Osborne et al (2000) Plasma Physics and Controlled Fusion **42** A175
[4]. C. Giroud et al Nuclear Fusion **53** (2013) 113025
[5]. M. Beurskens et al (2014) Nuclear Fusion **54** 043001
[6]. E. Joffrin et al this conference
[7]. E. Solano et al (2014) Proc. 41st EPS Conference (2014)
[8]. I. Nunes et al this conference
[9]. G. Saibene et al (2005) Nuclear Fusion **45** 297
[10]. G. Maddison et al (2014) Nuclear Fusion **54** 073016
[11]. R. Neu et al (2013) Physics of Plasmas **20** 056111
[12]. S. Bresinzek et al (submitted for publication)
[13]. A. Loarte et al (1998) Nuclear Fusion **38** 331
[14]. L. Frassinetti et al (submitted for publication)
[15]. A. Loarte et al (2002) Plasma Physics and Controlled Fusion **44** 1815–1844
[16]. B Sieglin et al 2013 Plasma Physics and Controlled Fusion **55** 124039
[17]. C. Challis et al this conference
[18]. M. Beurskens et al (2013) Plasma Physics and Controlled Fusion **55** 124043
[19]. P. Snyder (2014) Nuclear Fusion **44** 320–328
[20]. C. Maggi et al this conference

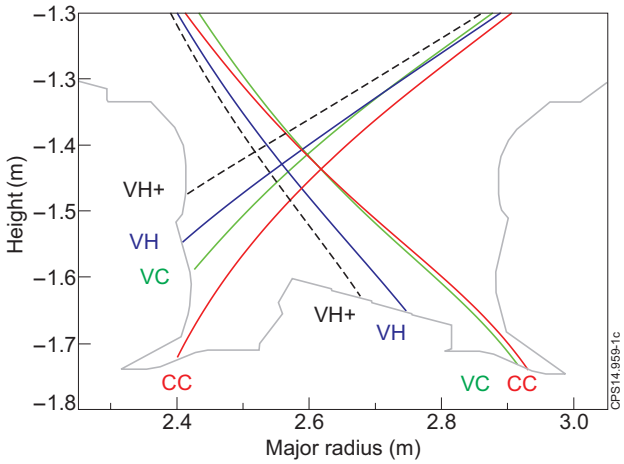

Figure 1: Divertor magnetic topology for the experiments described in this paper. Configuration names are AB/LT=A/B: Inner/ outer strike point location (vertical, corner or horizontal), LT: low-δ, HT: high-δ.

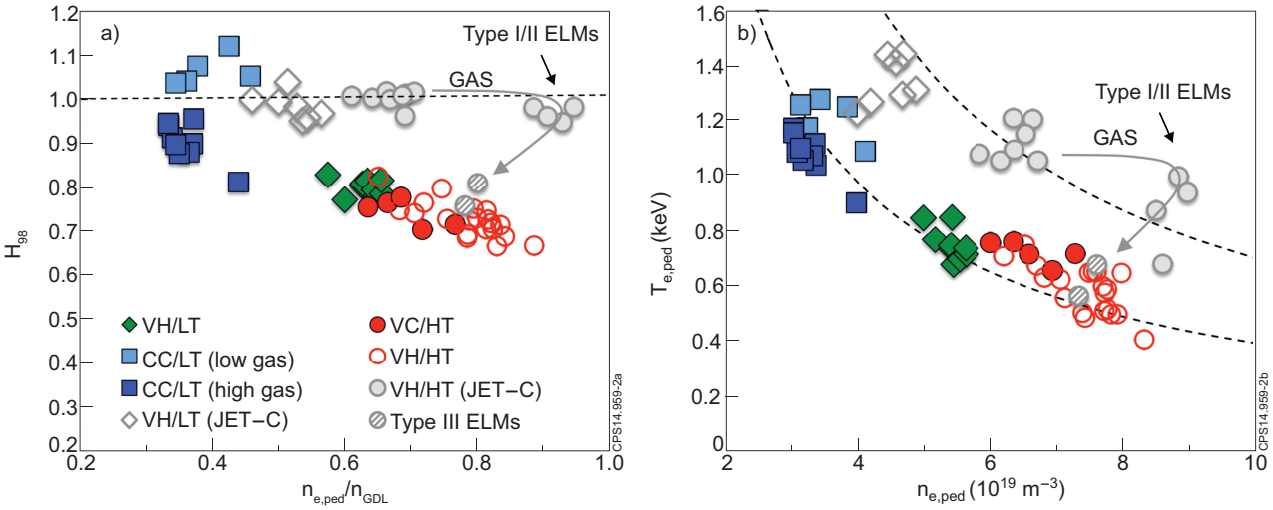

Figure 2: (a) H_{98} versus $n_{e,ped}/n_{GDL}$ for discharges in various divertor configurations (naming convention described in Figure 1) for $I_p = 2.5$MA, $P_{NBI} = 14$–20MW, for low and high triangularity plasmas and different values of gas fuelling. Data for JET-C are also included. (b) $T_{e,ped}$ versus $n_{e,ped}$ for the data shown in Figure 2(a). Lines are shown to guide the eyes during a gas scan at high-δ in JET-C. For the gas puffing rates corresponding to the high and low gas discharges shown here see Figure 4.

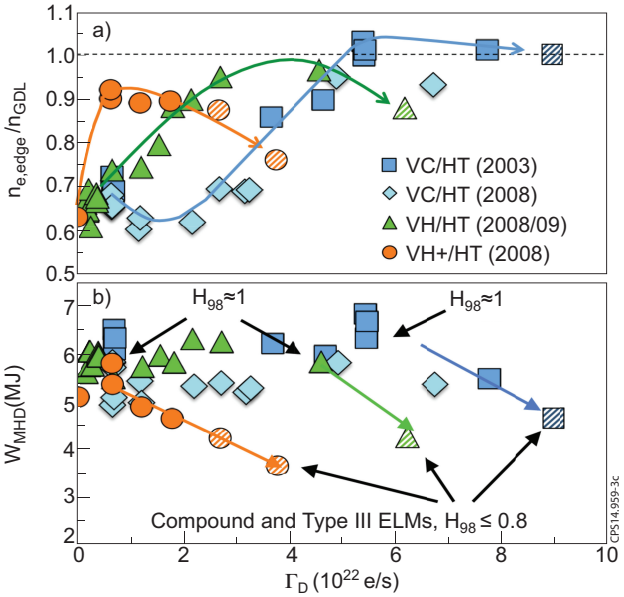

Figure 3: Variation of (a) n_e/n_{GDL}, and (b) W_{MHD} with gas injection rate for a selection of high-δ pulses with different divertor geometries in JET-C. Lines are drawn to guide the eyes. Configuration names as in Figure 1.

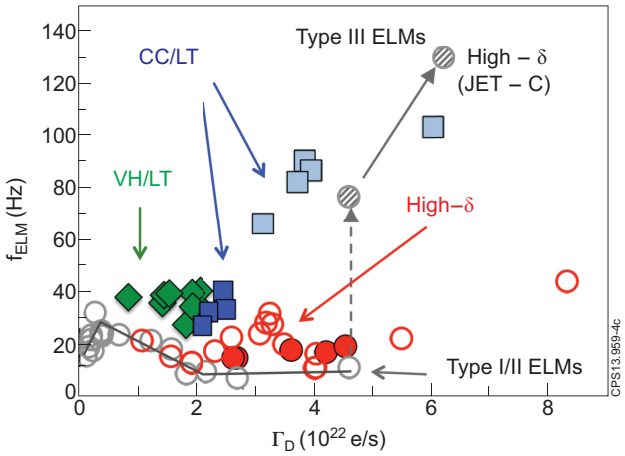

Figure 4: f_{ELM} variation with gas injection rate for the data set shown in Figure 2.

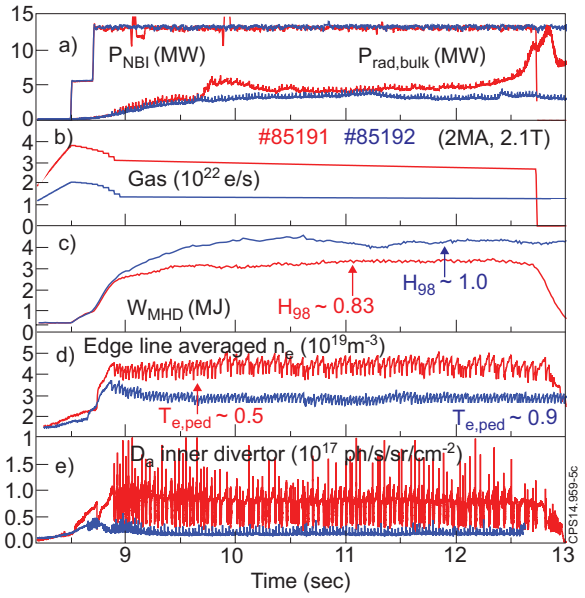

Figure 5: Time histories of several plasma parameters for two low-δ discharges (2MA, 2.1T) with the same divertor geometry (corner configuration) but different gas puffing rate.

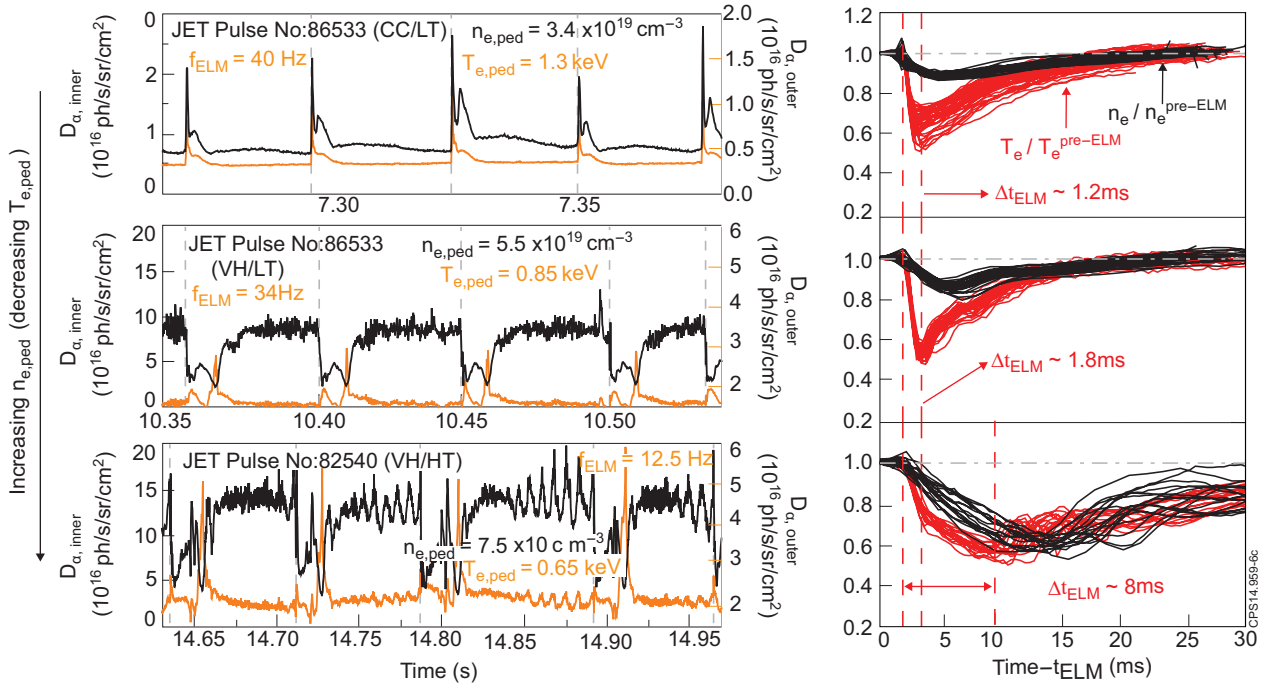

Figure 6: ELM dynamics as seen by the Dα (inner and outer divertor) signals for three discharges (2.5MA, $P_{NBI} \approx 15.5$MW) with increasing ne,ped: (a) Pulse No: 86533 (CC/LT), (b) Pulse No: 86533 (VH/LT), (c) Pulse No: 82540 (VH/HT). ELM synchronized time evolution of T_e (red) and n_e (black) at the pedestal top, with the data normalized to the pre-ELM value, is shown in the second column for the three discharges.

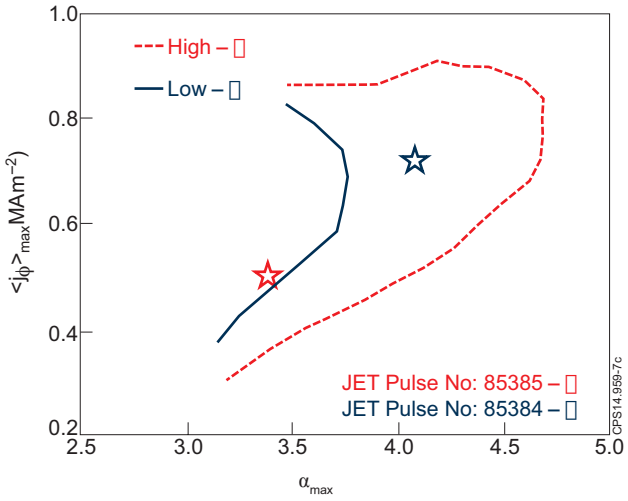

Figure 7: The P-B mode stability diagrams, for a low density, low-δ (CC/LT, Pulse No: 85385) and a high-δ (VC/HT, Pulse No: 85385) JET-ILW discharges (2.5MA, $P_{NBI} = 20$MW).